*Desalination and Water Treatment*
www.deswater.com

doi: 10.5004/dwt.2021.26934

218 (2021) 210–219
April

# Nitrobenzene removal by novel pillared kaolinite-catalyzed Fenton-like reaction

Yuanjing Zhang, Sihai Hu*, Xiaohui Mi, Rui Zhang, Ran Sun, Yaoguo Wu*

*School of Chemistry and Chemical Engineering, Northwestern Polytechnical University, Xi'an 710072, China, emails: mirrorzyj@163.com (Y. Zhang), husihai@nwpu.edu.cn (S. Hu), mixh@mail.nwpu.edu.cn (X. Mi), 978856229@mail.nwpu.edu.cn (R. Zhang), sunran@nwpu.edu.cn (R. Sun), wuygal@nwpu.edu.cn (Y. Wu)*

Received 14 June 2020; Accepted 14 December 2020

**ABSTRACT**

In this study, a novel metal-pillared kaolinite (KDF) Fenton-like catalyst was prepared via a two-step procedure involving intercalating and pillaring. The characterization results indicated that the interlayer spacing, specific surface area, pore area and volume were dramatically enhanced for KDF compared with raw kaolinite, and FeOOH crystals were present in the interlayer spaces of KDF. When KDF was used to catalyze the Fenton-like reaction for nitrobenzene (NB) degradation in the presence of $H_2O_2$, more than 85% of NB was removed. The influencing factors of $H_2O_2$ concentration, KDF dosage, NB initial concentration and reaction temperature as well the Fenton-like reaction mechanism were examined. The optimal conditions were determined to be: 10 mmol/L $H_2O_2$, 75 mg/L NB, and KDF dosage of 1.0 g/L. The first-order kinetic reaction rate constants at different temperatures were fitted by the Arrhenius equation and the activation energy ($E_a$) was calculated to be 36.34 kJ/mol. The experimental results in the presence of a free radical scavenger showed that the NB degradation mechanism catalyzed by KDF was mainly due to the generation of free hydroxyl radicals. The low percentage of leaching Fe-containing active components showed that the KDF catalyst has good stability, suggesting its potential application in environmental remediation.

*Keywords:* Pillared kaolinite; Catalysis; Fenton-like; Nitrobenzene; Hydroxyl radical

## 1. Introduction

Nitrobenzene (NB), as one of the most representative nitroaromatic compounds, is extensively used in the organic synthesis industry for the manufacture of dyes, spices and explosives [1–3]. NB is known to be highly toxic to organisms and plants, and resistant to microbial degradation [4–6]. For this reason, NB is deemed a priority control pollutant by many countries. For instance, the U.S. Environmental Protection Agency (EPA) recommends that NB levels in lakes and water streams should be no more than 17 mg/L to avoid potential health effects by drinking water or eating contaminated fish [7], and the discharge standards set by China have a maximum allowed concentration of 20 μg/L in the environment [8]. However, because of industrial and agricultural activities, the concentration of NB in some released wastewater can reach up to 35 mg/L [9,10]. Hence, minimizing the severe pollution caused by NB due to its extensive use, high toxicity and chemical stability in surface water or/and groundwater through efficient approaches has received great attention recently.

At present, a variety of methods are utilized for NB decomposition, especially advanced oxidation processes, such as the Fenton process, ozonation and catalytic wet oxidation [11,12]. Among these methods, the Fenton process is widely applied in the decomposition of persistent organic pollutants in drinking water and wastewater. Recently, a Fenton-like reaction was also proved to be an effective method for degradation of nitroaromatic compounds because of the advantages of high mineralization efficiency,

* Corresponding authors.

easy implementation and cost-saving [13–15]. Both in the Fenton and Fenton-like process, the catalyst plays an important role since it reacts with hydrogen peroxide ($H_2O_2$) to generate highly reactive hydroxyl radicals (•OH), which may react with the target pollutants. According to the phase of catalyst, Fenton/Fenton-like process can be divided into two categories, heterogeneous and homogeneous reactions [16]. Some transition metal ions, such as $Fe^{3+}$, $Fe^{2+}$, $Cu^{2+}$ and $Mn^{2+}$, are usually employed as homogenous catalysts [7]. Although significant benefits were obtained in the degradation of organic pollutants, the homogeneous Fenton/Fenton-like process is not considered as an economical and environment-friendly process due to the loss of catalysts and the subsequent pollution to the water system.

Heterogeneous catalysts in Fenton and Fenton-like processes have more advantages in the decomposition of organic contaminants than the homogeneous species due to their reusability and extensive sources. Numerous materials have been used in heterogeneous Fenton or Fenton-like processes, including Fe-containing compounds, activated carbon, transition metals, clay minerals, etc. [17–22]. Clay minerals and their modified products such as montmorillonite, kaolinite and zeolite were demonstrated to be efficient catalysts for the decomposition of organic pollutants [4,8,23,24]. For instance, Fe pillared montmorillonite clay displayed a special promoting effect in hydroxyl radical generation due to its abundant hydroxyl groups on the surface and presented excellent efficiency in catalytic Fenton-like reaction [25,26]. However, montmorillonite and its pillared derivatives easily swell and are difficult to precipitate in an aqueous solution, which severely limits their use as catalysts in the Fenton-like method [27]. Although it is layered mineral-like montmorillonite, kaolinite is non-swelling in water and has a higher porosity content and surface area that can be readily hydroxylated [28,29]. Therefore, using pillared kaolinite to catalyze the Fenton-like reaction may overcome the shortcomings of pillared montmorillonite catalysts and broaden the applications of the Fenton-like method. However, it is difficult to perform pillaring modification with commonly-used ion exchange methods due to few exchangeable cations between the kaolinite layers and the presence of strong interlayer hydrogen bonding. Hence, only a few studies have focused on pillared kaolinite and its application for catalyzing the Fenton-like reaction to remove NB from wastewater.

Hence, based on the potential superior characteristics of kaolinite as a Fenton-like catalyst, in this study, a new type of metal-pillared kaolinite (KDF) was prepared by intercalating and pillaring processes. Using NB as the target pollutant and the removal percentage as the evaluation index, the use of KDF as a catalyst for the Fenton-like reaction was evaluated, and the mechanism and influencing factors were simultaneously studied.

## 2. Materials and methods

### 2.1. Materials

Kaolinite, which is a certified reference material (Approved by State Bureau of Technical Supervision, China) obtained from the Geological Survey of Jiangsu Province (Nanjing, China), consisting of about 96% of kaolinite [26]. The chemical reagents of ferric nitrate, NB and $H_2O_2$ (30%, v/v) were purchased from the Xi'an Chemical Corporation (Xi'an, China), and dimethyl sulfoxide (DMSO) (>99.8%) was obtained from Shanghai Macklin Biochemical Co., Ltd. All other chemicals used in this study were of analytical grade. Deionized water (resistance > 18 MΩ) was used to prepare all reagents.

### 2.2. Preparation of KDF

The Fenton-like catalyst of pillared kaolinite (KDF) was prepared by the hydrolysis precipitation method. Specifically, 10 g kaolinite was added to the mixed solvent system of 10 mL deionized water and 90 mL DMSO and stirred under 80°C. After a reaction of 24 h, the solid was separated through centrifugation, and washed repeatedly with ethanol and dried under 40°C to obtain the precursor of kaolinite-DMSO (KD) for further use.

The prepared KD was ground into a powder. $Fe^{3+}$ with a concentration of 0.1 mol/L and aqueous ethanol solution were mixed in a certain volume ratio to obtain a 50 mL homogeneous solution. Then, the KD powder was added to the solution and magnetically stirred for 24 h at the temperature of 25°C. Strong ammonia water was slowly added to the system until the pH was 8 and then the system was allowed to settle for 12 h. The reaction system was subjected to centrifugal separation. The solid was washed with deionized water several times until the conductivity was constant and then dried at 80°C. It was then subjected to grinding, followed by calcination at 200°C for 3 h to obtain the composite of KDF (kaolinite-DMSO-$Fe(NO_3)_3{\cdot}9H_2O$).

### 2.3. Batch experiments

Using NB as the target pollutant and the removal percent as the evaluation index, an NB stock solution was prepared by dissolving 0.4 g NB in 1.0 L of deionized water. The working solutions with designed concentrations of the experiment were prepared by diluting the stock solution.

The catalytic Fenton-like reaction was carried out in a 250 mL glass reactor. The pH of 100 mL aqueous nitrobenzene solution was adjusted to 3.0 ± 0.05 by adding dilute $H_2SO_4$ solution or NaOH solution. Next, 1.0 mL of $H_2O_2$ solution with a concentration of 1.0 mol/L was added and stirred by a magnetic stirrer. Then, 0.1 g of prepared catalyst sample was added. Sample aliquots of 5.0 mL were extracted at various time points and centrifuged. The supernatant was transferred to a 5.0 mL glass reagent bottle which was sealed and refrigerated until further use. At each sampling, the pH value of the reaction system was measured. The procedure for the control experiment of adsorption was the same as above, except that no $H_2O_2$ solution was added.

### 2.4. Analysis and characterization

Scanning electron microscopy (SEM; VEGA 3 LMH, TESCAN, Czech) was used to view the surface characteristics and morphology of raw kaolinite and KDF, and energy-dispersive X-ray spectra (EDS) were obtained using Oxford INCA X-Act equipment in SEM. X-ray diffraction (XRD) spectra were recorded over the range of $2\theta = 10°\sim80°$ by powder diffractometer (Model D8, Bruker, Germany) with

Cu $K_{\alpha 1}$ radiation (0.154 nm). The instrument was operated with 40 kV and 30 mA at a scanning speed of 2°/min (2θ). Fourier-transform infrared spectroscopy (FTIR) was performed over the wavenumber range of 4,000–400 $cm^{-1}$ using a Nicolet iS10 Magna-IR Spectrometer (Nicolet Instrument Corporation, USA). The specific surface area, porosity and pore size of samples were measured by a Brunauer–Emmett–Teller (BET) instrument 3H-2000PS2 (BeiShiDe Instrument, China).

NB concentrations were determined using high-performance liquid chromatography equipped with a Waters Symmetry C18 column (150 mm × 4.6 mm i.d., 5.0 μm). The mobile phase was a mixture of methanol and 5 mM $H_3PO_4$ in the ratio of 3:2 (v/v) [30]. The flow rate was set at 1.0 mL/min, and the detection wavelength was set to 267.5 nm. The samples were filtered through 0.45 μm filters and then 20 μL was injected manually through an injection port. All the prepared samples were taken for analysis immediately [31]. Fenton-like reactions were conducted in triplicate and only the data meeting the requirements were used.

The concentration of dissolved iron ions leached from the catalyst into the reaction solution was determined using atomic absorption spectrophotometry (Zeeman 2000 Series, Hitachi, Japan) with a detection limit of 0.004 mg/L [32]. The pH value of the solution was measured by a PHSJ-4A monitor (Shanghai, China).

## 3. Results and discussion

### 3.1. Catalyst characterization

To analyze the structure of the prepared KDF, FeOOH was prepared based on the method described in the literature [33,34]. As shown in the XRD patterns in Fig. 1a, the structure of KDF contained crystalline regions. After pillaring, the interlayer spaces of kaolinite expanded from 0.68 nm to 0.72 nm, as calculated by the Bragg equation. The FTIR spectrum presented in Fig. 1b indicates that the functional group composition of KDF did not change significantly compared with the original kaolinite. The SEM micrographs of kaolinite and KDF are shown in Figs. 1c and d. As seen from Fig. 1c, the kaolinite was an elongated flaky solid with an obvious rod-like morphology, and there were some rod-like agglomerates in the kaolinite sample. The SEM image of KDF in Fig. 1d indicates that, after pillar modification, there are no significant differences in terms of rod-like structure and the edges of kaolinite. This illustrates that pillaring modification does not change the basic surface structure of kaolinite. However, according to the results of EDS (Table 1), the Fe content was 4.45% in KDF, which remarkably increased after pillaring modification. As is known, the Fenton-like reaction is a complex reaction that proceeds via the activation of hydrogen

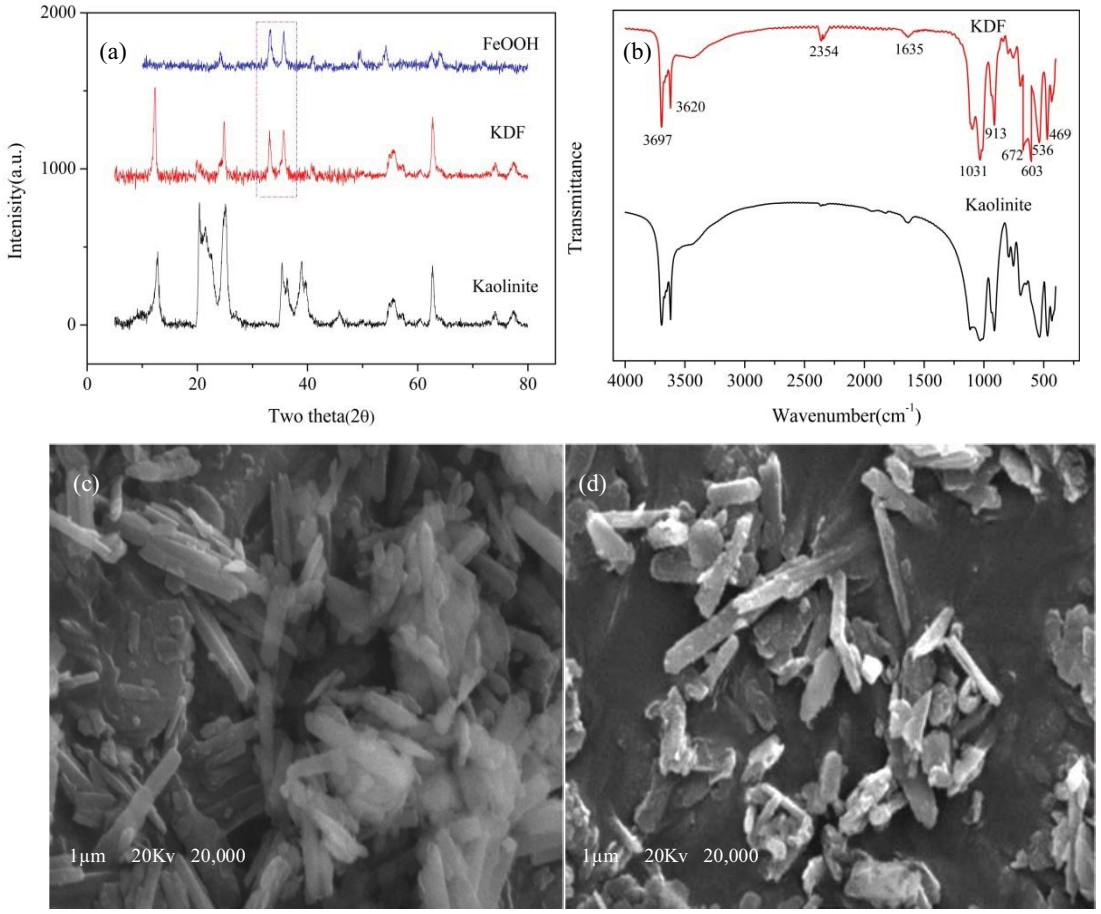


Fig. 1. (a) XRD, (b) FTIR, (c) SEM of kaolinite, and (d) KDF.

peroxide ($H_2O_2$) by ferrous ions to generate highly active hydroxyl radical (•OH) (Eqs. (1) and (2)), which then oxidizes and degrades the NB pollutant [35,36]. Hence, the increase in iron content and formation of FeOOH after pillaring of kaolinite can facilitate the Fenton-like reaction to generate more •OH. Moreover, the expanded interlayer space of kaolinite allows NB and hydroxyl radicals to enter the interior of kaolinite to improve the efficiency of catalytic reactions and prevent the loss of the catalyst [29].

$$Fe^{2+} + H_2O_2 \rightarrow Fe^{3+} + {}^{\bullet}OH + OH^- \quad (1)$$

$$Fe^{3+} + H_2O_2 \rightarrow Fe^{2+} + {}^{\bullet}O_2H + H^+ \quad (2)$$

Furthermore, the nitrogen adsorption–desorption results are shown in Table 2. These results indicate that after pillaring, the Langmuir specific surface area of kaolinite increased from 35.440 to 64.095 $m^2/g$. The BET specific surface area increased from 25.638 to 45.845 $m^2/g$ and the Barrett–Joyner–Halenda (BJH) specific surface area increased from 26.792 to 44.848 $m^2/g$, while the total pore volume increased from 0.0527 to 0.0849 $cm^3/g$. In addition, the average pore diameter of kaolinite after pillar modification decreased to about 7.5 nm with a narrower pore diameter distribution. Obviously, the pillaring modification significantly improved the surface features of kaolinite whose surface area and pore structure were increased, which is very important for the catalytic performance of kaolinite as a Fenton-like catalyst. Generally, according to the mechanism of the Fenton reaction, the increase in iron content, surface area and pore volume, and especially the formation of FeOOH in KDF, are beneficial to the Fenton-like catalytic effect for the removal of NB.

### 3.2. Catalytic performance of pillared kaolinite

The effect of initial pH on the degradation of NB by the KDF/$H_2O_2$ system was tested, and it was found that the optimal NB removal efficiency occurred when the pH was 3.05 ± 0.05 (Fig. S1). In order to verify the catalytic effect of KDF, the NB removal experiment was conducted in an aqueous solution ($H_2O_2$ concentration of 10 mmol/L) and also an NB adsorption experiment was conducted (without $H_2O_2$), using KDF or raw kaolinite with a pH of 3.0 ± 0.05, KDF or kaolinite content of 1.0 g/L, and an initial NB concentration of about 65.0 mg/L (actual measured concentration 64.31, 64.83, 66.14 and 65.12 mg/L for KDF, kaolinite, kaolinite with $H_2O_2$, and KDF with $H_2O_2$). The results are shown in Fig. 2 with the relative errors lower than ±5%. For the single kaolinite or KDF, and kaolinite/$H_2O_2$ system, the removal rates of NB were less than 10%, mainly due to the adsorption of kaolinite and KDF which are porous materials. On the other hand, the removal percentage of NB in the KDF catalytic system reached 89%. Hence, the results from the control experiments clearly show that the increased removal of NB using KDF for the Fenton-like reaction was mainly due to its catalytic effect. Therefore, pillared kaolinite significantly increased the NB removal efficiency of the Fenton-like reaction.

Table 1
Elements weight composed of kaolinite and KDF

| Samples | O (%) | Al (%) | Si (%) | Fe (%) | Total (%) |
|---|---|---|---|---|---|
| Kaolinite | 47.19 | 24.64 | 28.17 | – | 100 |
| KDF | 49.72 | 21.81 | 24.02 | 4.45 | 100 |

### 3.3. Influencing factors of the Fenton-like reaction catalyzed by KDF

#### 3.3.1. $H_2O_2$ concentration

The initial concentration of $H_2O_2$ was varied from 0.5~20.0 mmol/L to determine the optimal initial $H_2O_2$ concentration during the catalytic Fenton-like reaction, with the other reaction conditions as described in the batch experiment. The results are shown in Fig. 3. The results in Fig. 3a indicate that, as the initial $H_2O_2$ concentration increased from 0.5~5.0 mmol/L, both the final removal

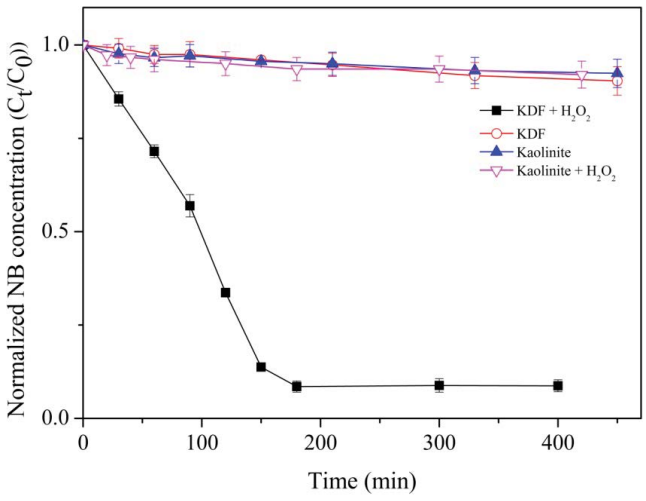


Fig. 2. Catalytic effect of KDF to remove NB by Fenton-like reaction.

Table 2
Specific surface area and pore analysis of kaolinite and KDF

| Samples | BET ($m^2/g$) | Langmuir ($m^2/g$) | BJH ($m^2/g$) | Pore volume ($cm^3/g$) | Pore size (Å) |
|---|---|---|---|---|---|
| Kaolinite | 25.638 | 35.440 | 26.792 | 0.0527 | 91.255 |
| KDF | 45.845 | 64.095 | 44.848 | 0.0849 | 79.520 |

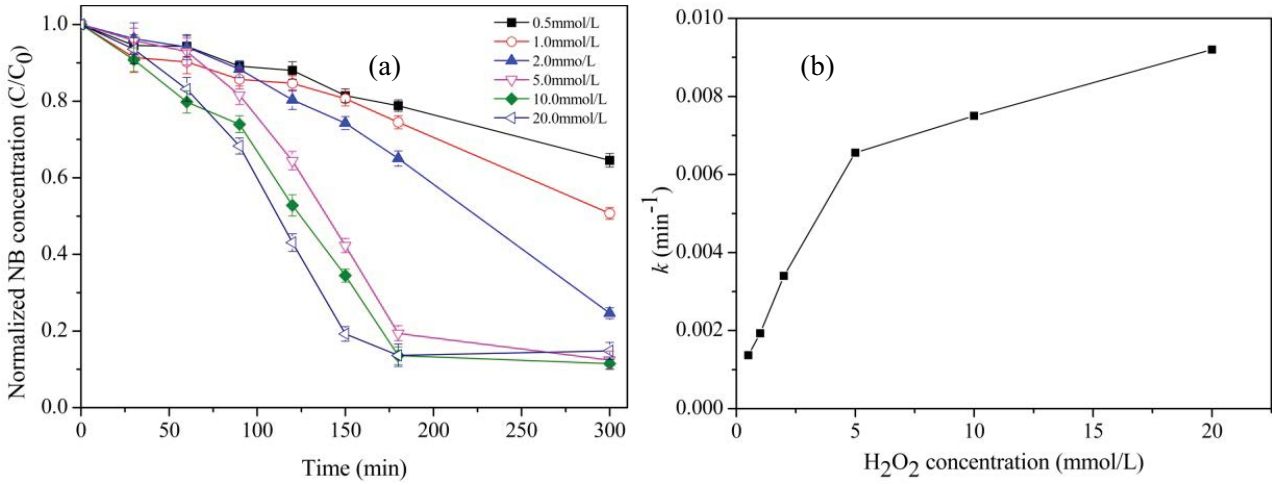


Fig. 3. Initial $H_2O_2$ concentration effects on Fenton-like reaction (a) and kinetic constants (b) catalytic by KDF.

percentage and the degradation rate of NB rapidly increased. However, from 5.0~20.0 mmol/L, increasing the initial $H_2O_2$ concentration had little effect on the final removal percentage of NB or the time to reach reaction equilibrium, and it only slightly affected the NB degradation rate. Moreover, there was a clear inflection point between the two concentrations over the studied range of concentrations (Fig. 3a).

The removal reaction can be described as a pseudo-first-order reaction with respect to NB concentration as given in Eq. (3):

$$v = -\frac{dC_t}{dt} = k \times C_t \tag{3}$$

where $k$ is the observed first-order reaction rate constant, which is the slope of the regression lines obtained by plotting a natural logarithm graph with respect to NB concentration and reaction time according to Eq. (4):

$$-\ln\left(\frac{C_t}{C_0}\right) = k \times t \tag{4}$$

where $t$ is the reaction time, $C_0$ is the initial NB concentration, and $C_t$ is the NB concentration at $t$ time, respectively. A linear regression of the first-order kinetic Eq. (4) was performed for each group of data.

The first-order reaction kinetic model was used to fit the NB concentration change under different $H_2O_2$ concentrations, and the relationship between the initial $H_2O_2$ concentration and the reaction rate constant $k$ is shown in Fig. 3b. The change in the reaction rate constant also suggests that there is an optimal $H_2O_2$ concentration with an initial concentration of pollutants at given conditions. Under the experimental conditions, the value of $k$ increased sharply from 0.5 to 5.0 mol/L while the $k$ increased moderately from 5.0 to 20.0 mmol/L (Fig. 3b).

Similar phenomena have been found in the degradation of other organic pollutants by Fenton or Fenton-like reaction. For instance, the experiments carried out by Li et al. [37] revealed that when using an Al/Fe-UV method to degrade the azo dye X-3B, increasing the $H_2O_2$ concentration to a certain extent had only a small impact on the degradation rate. Several studies have indicated that a high $H_2O_2$ concentration will react with the generated free radicals ($^{\bullet}OH$) as shown in Eqs. (5)~(7):

$$H_2O_2 + {}^{\bullet}OH \rightarrow H_2O + HO_2^{\bullet} \tag{5}$$

$$HO_2^{\bullet} + {}^{\bullet}OH \rightarrow H_2O + O_2 \tag{6}$$

$$HO^{\bullet} + {}^{\bullet}OH \rightarrow H_2O_2 \tag{7}$$

Such reactions can weaken the oxidation capability of the Fenton-like system and affect the utilization efficiency of $H_2O_2$ [25,38]. Thus, increasing the initial $H_2O_2$ concentration had little effect on the Fenton-like catalytic effect.

### 3.3.2. Catalyst KDF dose

The KDF dose of 0.5~1.5 g/L was selected to carry out the catalytic Fenton-like degradation of NB and other reaction conditions were maintained as described in the batch experiments. The results in Fig. 4a show that the catalyst dosage slightly affected both the final removal percentage of NB and the shape of the degradation curve. This can also be proved by the first-order reaction rate constant $k$ shown in Fig. 4b. When the dose of KDF increased from 0.5 to 1.5 g/L, the constant $k$ increased from $8.93 \times 10^{-3}$ to $13.63 \times 10^{-3}$.

The results suggest that 0.5 g/L of KDF was enough to catalyze the Fenton-like reaction for the degradation of NB. The main reason is attributed to the large specific surface area and highly porous structure of KDF catalyst, whose characteristics were improved greatly after intercalation and pillar modification. Hence, a higher KDF concentration transferred more $H_2O_2$ and NB molecules from the liquid phase to the solid–liquid interface within the same period. This increased the probability of contact between NB and the hydroxyl radicals generated during $H_2O_2$-catalyzed

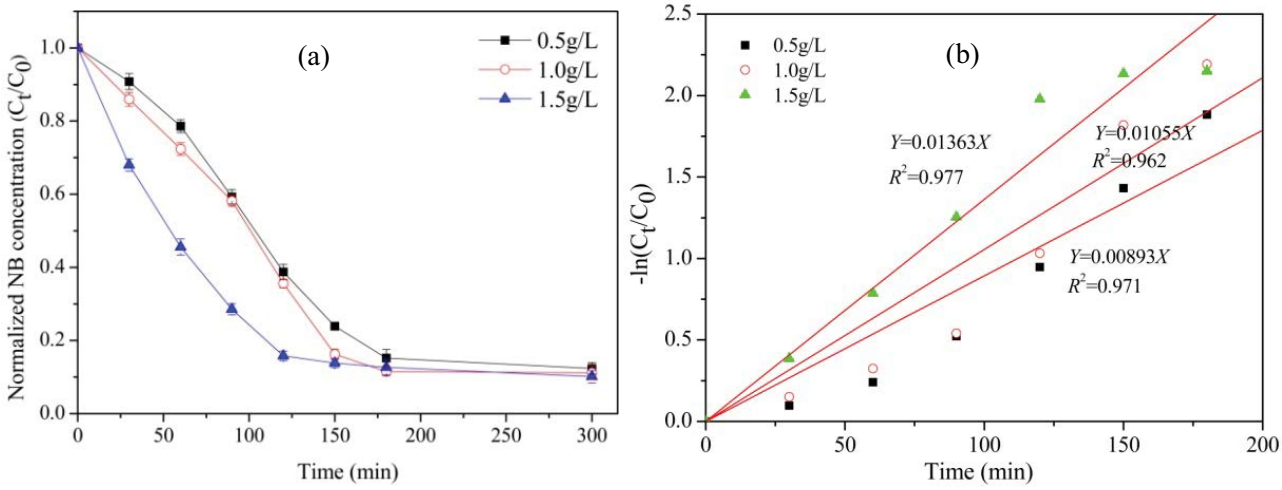


Fig. 4. Catalyst dosage effects on Fenton-like reaction (a) and kinetics (b) ($n$ = 8; $R^2_{0.05}$ = 0.707; $R^2_{0.01}$ = 0.834).

decomposition, which further accelerated the degradation of NB [39,40].

*3.3.3. NB concentration*

The concentration of NB was varied from 25.0~100.0 mg/L in the Fenton-like reaction, and its effects on the catalytic Fenton-like degradation are shown in Fig. 5a. The data shows that the NB concentration had little effect on the equilibrium of catalytic degradation since the equilibrium removal rates of NB were 83% (25 mg/L), 89% (50 mg/L), 89% (70 mg/L), and 89% (100 mg/L). Apparently, the final removal percent of low-concentration NB was lower than that of high-concentration NB. This phenomenon could be due to the fact that, under the same catalyst dose and $H_2O_2$ concentration, the number of •OH free radicals generated by the catalytic decomposition of $H_2O_2$ were nearly the same. Thus, when the NB concentration was low, due to the higher •OH/NB ratio, most NB molecules in water quickly decomposed into small-molecule organic acids, such as acetic acid and oxalic acid [7,9]. These substances rapidly accumulated and reacted with •OH to form other free radical species with lower activities, which decreased the oxidizing capability of the system and lowered the removal efficiency of NB [41–43].

At NB concentrations from 25~100 mg/L, the reaction rate constant $k$ decreased with the increase in concentration (Fig. 5b). However, at NB concentrations from 50~75 mg/L, the reaction rate constant $k$ remained nearly the same because the types and concentrations of intermediate products in the reaction system were similar. Ruppert et al. [44] reached a similar conclusion when examining the degradation effect of hydroxyl radicals on aromatic hydrocarbons with different structures, that is, the oxidizing ability of hydroxyl free radicals was affected by the pollutant species. In addition, when the NB concentration was low, $H_2O_2$ will compete with •OH due to the high $H_2O_2$/NB ratio. The reaction between $H_2O_2$ and •OH can form less-active $HO_2^{\bullet}$ free radicals, which decreases the oxidative degradation of NB [45,46].

*3.3.4. Reaction temperature*

The catalytic Fenton-like reactions were carried out at three temperatures of 300, 308, and 313 K adjusted by a constant-temperature water bath, with the other reaction conditions the same as described above. The results are shown in Fig. 6. It is clearly observed that temperature only slightly affected the equilibrium of the catalytic removal of NB by the Fenton-like reaction since the percent removal of NB was nearly the same once equilibrium was reached. However, the temperature significantly affected the reaction process and time to reach equilibrium, which is consistent with the trends observed by Ramirez et al. [47] who used Fe-pillared soapstone to catalyze the Fenton-like degradation of orange II dye. The results also suggest that a higher reaction temperature accelerated the catalytic Fenton-like degradation of NB. However, the research conducted by Najjar et al. [25] showed that the slower degradation of organic matter at lower temperatures was not due to a reduction in the oxidizing capability of $H_2O_2$, but rather due to a reduction in the rate of free radical generation. An increase in the reaction temperature can accelerate the mass transfer of molecules, allowing the free radicals to contact more organic molecules before annihilation or deactivation, thereby promoting the complete degradation of organics and the efficient use of free radicals.

The first-order reaction equation was used to fit the reaction kinetics data at different temperatures, and the results are shown in Fig. 6b. The slope of each fitted linear line corresponds to the rate constant $k$ at each temperature, as presented in Table 3. As the reaction temperature increased, the reaction rate constant became larger. The relationship between the reaction rate constant and the temperature did not show a linear relationship (Fig. 6c), but it could be described by the Arrhenius equation:

$$k = k_0 \cdot \exp\left(\frac{-E_a}{RT}\right) \quad (8)$$

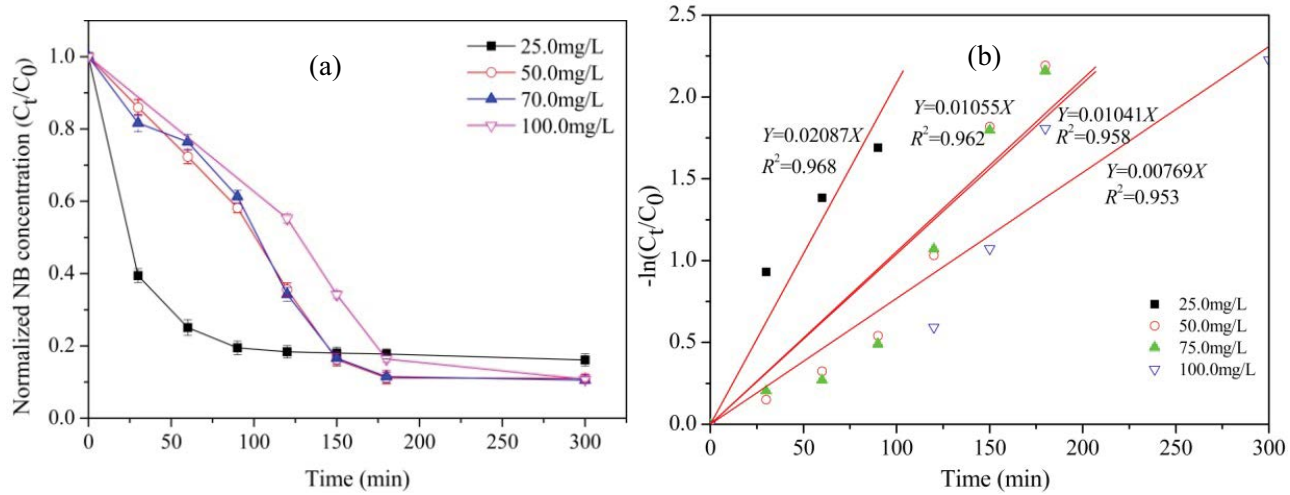


Fig. 5. Initial NB concentration effects on Fenton-like reaction (a) and kinetics (b) catalytic by KDF ($n$ = 8; $R^2_{0.05}$ = 0.707; $R^2_{0.01}$ = 0.834).

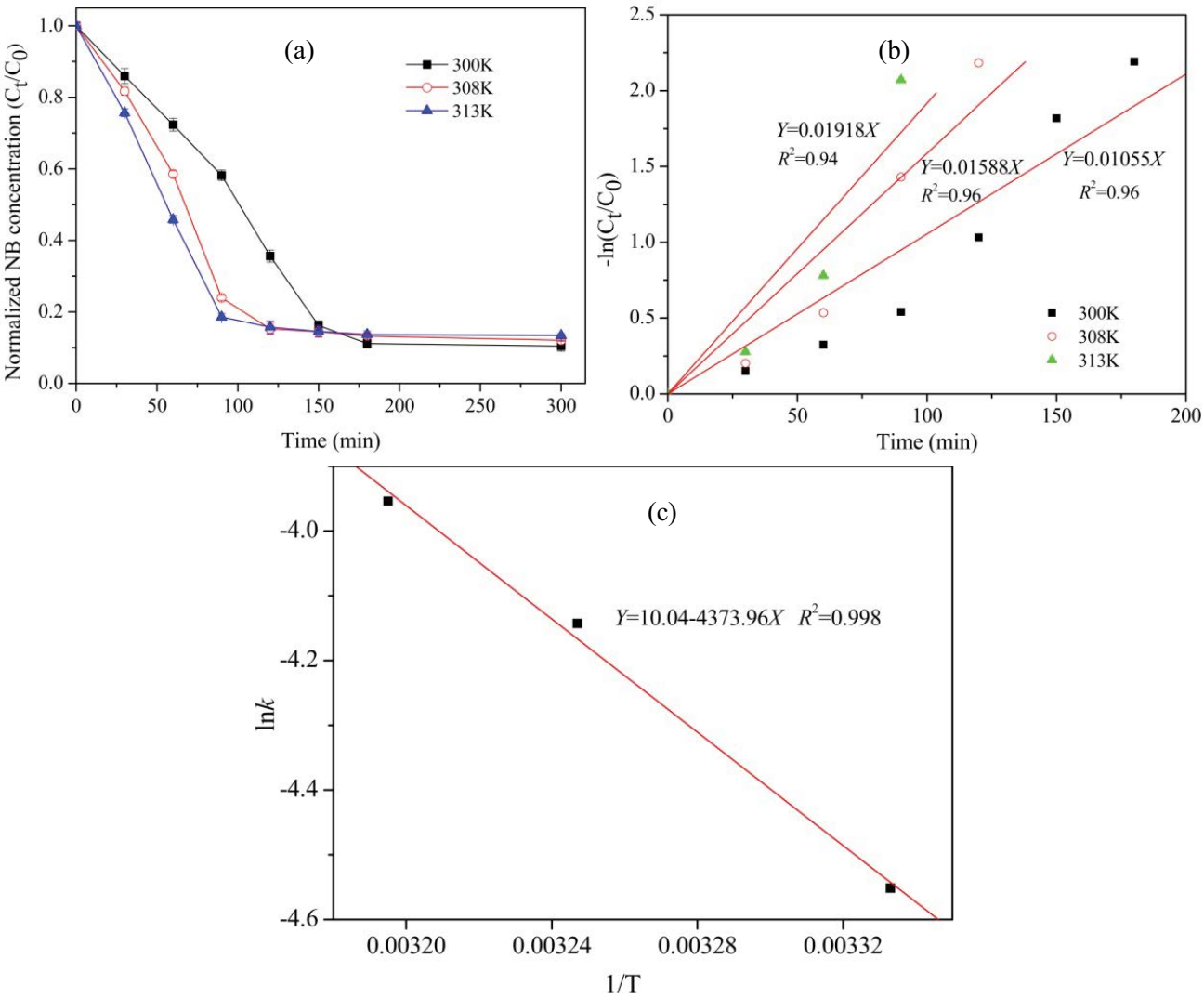


Fig. 6. Temperatures effect on Fenton-like reaction (a), kinetics (b) and Arrhenius kinetic constants (c) ($n$ = 8; $R^2_{0.05}$ = 0.707; $R^2_{0.01}$ = 0.834; $n$ = 3; $R^2_{0.05}$ = 0.997; $R^2_{0.01}$ = 1).

Table 3
First-order kinetics fitting of rate constants at different temperatures

| $T$ (K) | $K$ ($s^{-1}$) | $R^2$ | $1/T$ | ln$k$ |
|---|---|---|---|---|
| 300 | 0.01055 | 0.96 | 0.003333 | –4.55163 |
| 308 | 0.01588 | 0.96 | 0.003247 | –4.14269 |
| 313 | 0.01918 | 0.94 | 0.003195 | –3.95389 |

where $E_a$ denotes the activation energy of the reaction. The equation can be converted into the following form after taking the natural logarithms of both sides:

$$\ln k = \ln k_0 - \left(\frac{E_a}{RT}\right) \quad (9)$$

As shown in Fig. 6c, ln$k$ and $1/T$ data from Table 3 were fit with a straight line whose slope was $E_a/R$. The linear data was substituted into the calculation, and the activation energy $E_a$ was calculated to be 36.34 kJ/mol. The activation energy is much lower than those of ordinary chemical reactions, which is in accordance with the characteristics of free radical reactions and indicates that free radicals participated in the catalytic Fenton-like removal of NB by KDF.

### 3.4. Regenerability and stability of KDF

The catalyst regeneration performance is crucially important for its practical application [28]. Therefore, this study examined the effect of reusing KDF catalyst on the properties of Fenton-like degradation of nitrobenzene, and the results are shown in Fig. 7a. It can be seen that the catalytic Fenton-like degradation of nitrobenzene achieved an excellent removal rate (87%) with three cycles, but the effect of extended time increased with the increase in a number of recycling. When used for the first time, after a short period of slow reaction (about 60 min), nitrobenzene was rapidly removed and the removal rate reached 84% after 180 min reaction. When used for the second time, the slow reaction period was significantly prolonged to 180 min, and the nitrobenzene removal rate was only 73% after 300 min, and the removal rate reached 87% after 420 min reaction. When used for the third time, the slow reaction period was similar to the second use, and the removal rate was 88% after 540 min reaction. The experimental results illustrated that the modified catalyst of KDF can be reused, although the catalytic efficiency was slightly reduced after cyclic utilization. This phenomenon is common in the experiments of heterogeneous Fenton-like degradation of organic pollutants. For instance, Catrinescu et al. [48] also found that the removal efficiency after recycling was reduced when pillared beidellite was used for the degradation of phenol pollutants.

Fig. 7b shows the variation in the concentration of dissolved Fe-containing components and pH values in the reaction system with an initial NB concentration of 50.0 mg/L, pH of 3.08, $H_2O_2$ concentration of 10 mmol, and KDF dose of 1.0 g/L. Over the process of reaction, the maximum dissolved Fe concentration of about 1.1 mg/L was observed at 30 min. This indicates that the modified catalyst of KDF has good stability which can reduce iron leaching in Fenton-like reaction. The pH first slightly increased and then decreased, but the overall pH ranged from 2.8 to 3.25, which is within the optimal pH range (~3.0) for the Fenton-like reaction. Generally, the survey results showed that the KDF catalyst was not only stable but also had high catalytic activity, which is a good potential heterogeneous catalyst for a Fenton-like reaction.

### 3.5. Catalytic mechanism of KDF

In order to further verify the presence of free radicals in the reaction system, heterogeneous Fenton-like reactions were carried out using two scavengers (ethanol and *tert*-butanol) of hydroxyl free radicals, and the results are shown in Fig. 8.

Obviously, when ethanol or *tert*-butanol was present in the system, the final percent removal of NB was significantly reduced. Compared with the NB adsorption by KDF, NB removal in the presence of ethanol or *tert*-butanol was mainly induced by adsorption by KDF. However, the experimental results in section 3.3.3 showed that the NB initial

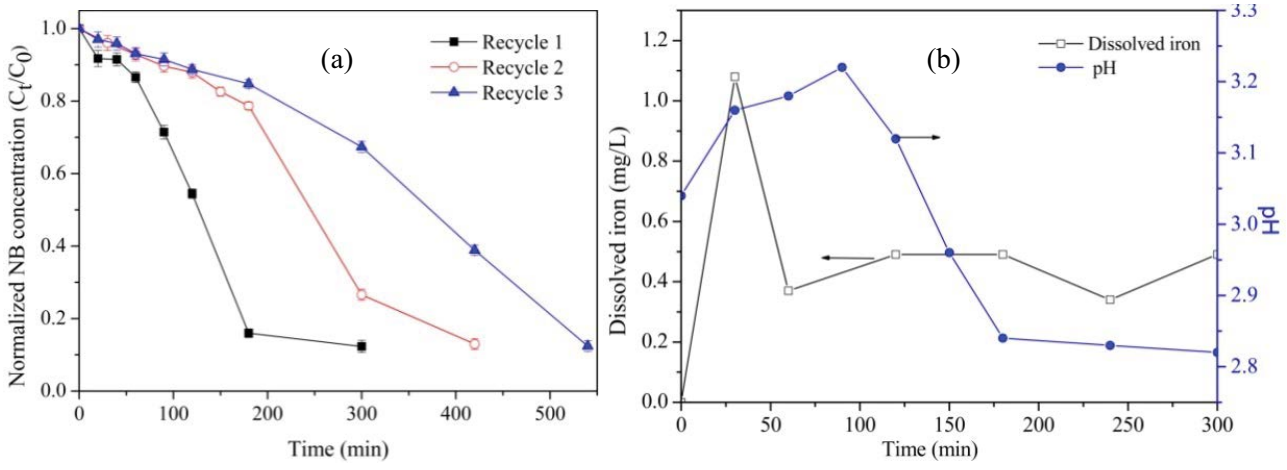


Fig. 7. Catalyst recycling (a) and dissolved iron ions as well as pH change (b) in Fenton-like reaction.

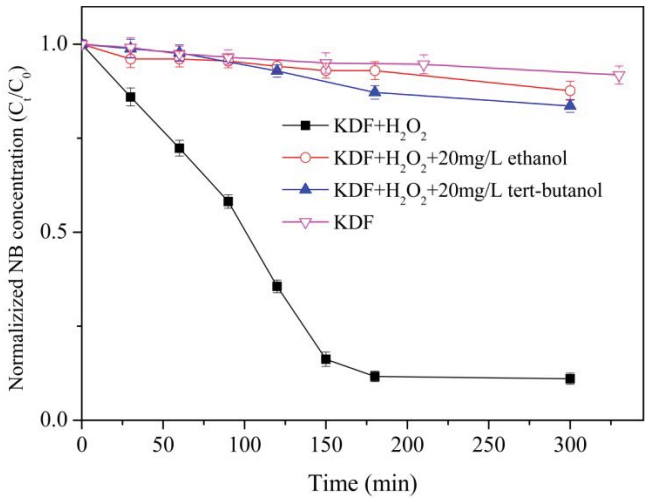


Fig. 8. Effects of free radical scavengers on NB removal by the Fenton-like reaction.

concentration did not significantly affect the equilibrium removal percent of NB [49,50]. Therefore, the sharp decrease in the percent removal of NB in the presence of ethanol or *tert*-butanol was not due to an increase in pollutant concentration in the system, but rather due to the rapid reaction between the two alcohols and •OH and the formation of inert species. Consequently, the experimental results indirectly verified that KDF can catalyze the Fenton-like degradation of NB mainly due to the presence of strongly oxidizing •OH free radicals generated during Fenton-like reaction.

## 4. Conclusions

A new type of metal-pillared kaolinite (KDF) Fenton-like catalyst was prepared by intercalation and pillaring processes and its catalytic activity in Fenton-like reaction to remove NB was tested. The main conclusions are as follows:

- The structural characteristics of kaolinite were improved by pillaring with metal ions, and the interlayer spacing, specific surface area, pore area and pore content of KDF were significantly enhanced.
- KDF had a significant catalytic effect on the degradation of NB in an aqueous solution by the Fenton-like reaction and the removal percent of NB reached more than 85% under the optimal experimental conditions. The degradation was mainly due to the generation of hydroxyl radicals in the Fenton-like system. The activation energy $E_a$ of NB degradation was 36.34 kJ/mol and the reaction conditions strongly affected the efficiency of Fenton-like process catalyzed by KDF.

## Acknowledgments

The authors gratefully acknowledge the financial support by the National Natural Science Foundation of China (Nos. 41502240 and 41601338), the Natural Science Basic Research Plan in Shaanxi Province of China (Nos. 2020JM-110 and 2018JQ4019), the Fundamental Research Funds for the Central Universities (No. 3102018zy042), and the National Training Program of Innovation and Entrepreneurship for Undergraduates (S201910699176).

## References

[1] P.S. Majumder, S.K. Gupta, Hybrid reactor for priority pollutant nitrobenzene removal, Water Res., 37 (2003) 4331–4336.
[2] S.H. Hu, H.R. Yao, K.F. Wang, C. Lu, Y.G. Wu, Intensify removal of nitrobenzene from aqueous solution using nano-zero valent iron/granular activated carbon composite as Fenton-like catalyst, Water Air Soil Pollut., 226 (2015) 1–13.
[3] H.Q. Zhao, Q. Liu, Y.X. Wang, Z.Y. Han, Z.G. Chen, Y. Mu, Biochar enhanced biological nitrobenzene reduction with a mixed culture in anaerobic systems: short-term and long-term assessments, Chem. Eng. J., 351 (2018) 912–921.
[4] Y. Sun, Z.X. Yang, P.F. Tian, Y.Y. Sheng, J. Xu, Y.-F. Han, Oxidative degradation of nitrobenzene by a Fenton-like reaction with Fe-Cu bimetallic catalysts, Appl. Catal., B, 244 (2019) 1–10.
[5] Z.X. Qiao, R. Sun, Y.G. Wu, S.H. Hu, X.Y. Liu, J.W. Chan, Microbial heterotrophic nitrification-aerobic denitrification dominates simultaneous removal of aniline and ammonium in aquatic ecosystems, Water Air Soil Pollut., 231 (2020) 3, https://doi.org/10.1007/s11270-020-04476-3.
[6] Z.X. Qiao, Y.G. Wu, J. Qian, S.H. Hu, J.W. Chan, X.Y. Liu, R. Sun, W.D. Wang, B. Zhou, A lab-scale study on heterotrophic nitrification-aerobic denitrification for nitrogen control in aquatic ecosystem, Environ. Sci. Pollut. Res., 27 (2020) 9307–9317.
[7] D.A. Nichela, A.M. Berkovic, M.R. Costante, M.P. Juliarena, F.S. García Einschlag, Nitrobenzene degradation in Fenton-like systems using Cu(II) as catalyst. Comparison between Cu(II)- and Fe(III)-based systems, Chem. Eng. J., 228 (2013) 1148–1157.
[8] H.T. Duan, Y. Liu, X.H. Yin, J.F. Bai, J. Qi, Degradation of nitrobenzene by Fenton-like reaction in a $H_2O_2$/schwertmannite system, Chem. Eng. J., 283 (2016) 873–879.
[9] W.K. Kirui, S. Wu, S. Kizito, P.N. Carvalho, R.J. Dong, Pathways of nitrobenzene degradation in horizontal subsurface flow constructed wetlands: effect of intermittent aeration and glucose addition, J. Environ. Manage., 166 (2016) 38–44.
[10] J.-H. Wu, F. Zhang, Rapid aerobic visible-light-driven photo-reduction of nitrobenzene, Sci. Total Environ., 710 (2020) 136322, https://doi.org/10.1016/j.scitotenv.2019.136322.
[11] W.Z. Jiao, P.Z. Yang, W.Q. Gao, J.J. Qiao, Y.Z. Liu, Apparent kinetics of the ozone oxidation of nitrobenzene in aqueous solution enhanced by high gravity technology, Chem. Eng. Process, 146 (2019) 107690, https://doi.org/10.1016/j.cep.2019.107690.
[12] S. Chong, Y.L. Song, H. Zhao, G.M. Zhang, Enhanced degradation of nitrobenzene by combined ultrasonic irradiation and a zero-valent zinc catalyst, Desal. Water Treat., 57 (2016) 23856–23863.
[13] A.D. Bokare, W.Y. Choi, Review of iron-free Fenton-like systems for activating $H_2O_2$ in advanced oxidation processes, J. Hazard. Mater., 275 (2014) 121–135.
[14] M. Mohadesi, A. Shokri, Evaluation of Fenton and photo-Fenton processes for the removal of p-chloronitrobenzene in aqueous environment using Box–Behnken design method, Desal. Water Treat., 81 (2017) 199–208.
[15] M.-H. Zhang, H. Dong, L. Zhao, D.-X. Wang, D. Meng, A review on Fenton process for organic wastewater treatment based on optimization perspective, Sci. Total Environ., 670 (2019) 110–121.
[16] A. Mirzaei, Z. Chen, F. Haghighat, L. Yerushalmi, Removal of pharmaceuticals from water by homo/heterogonous Fenton-type processes – a review, Chemosphere, 174 (2017) 665–688.
[17] Y. Lü, J.F. Li, Y.M. Li, L.P. Liang, H.P. Dong, K. Chen, C.X. Yao, Z.F. Li, J.X. Li, X.H. Guan, The roles of pyrite for enhancing reductive removal of nitrobenzene by zero-valent iron, Appl. Catal., B, 242 (2019) 9–18.

[18] Q. Liu, X.Q. Bai, X.T. Su, B. Huang, B.J. Wang, X.L. Zhang, X.X. Ruan, W.M. Cao, Y.F. Xu, G.R. Qian, The promotion effect of biochar on electrochemical degradation of nitrobenzene, J. Cleaner Prod., 244 (2020) 118890, https://doi.org/10.1016/j.jclepro.2019.118890.
[19] L. Liu, S.S. Fan, Y. Li, Removal of methylene blue in aqueous solution by a Fenton-like catalyst prepared from municipal sewage sludge, Desal. Water Treat., 138 (2019) 326–334.
[20] B.B. Feng, Y.X. Wei, Y.N. Qiu, S.F. Zuo, N. Ye, Ce-modified AlZr pillared clays supported-transition metals for catalytic combustion of chlorobenzene, J. Rare Earths, 36 (2018) 1169–1174.
[21] K.V. Bineesh, D.-K. Kim, H.-J. Cho, D.-W. Park, Synthesis of metal-oxide pillared montmorillonite clay for the selective catalytic oxidation of $H_2S$, J. Ind. Eng. Chem., 16 (2010) 593–597.
[22] S.Ts. Khankhasaeva, S.V. Badmaeva, Removal of p-aminobenzenesulfanilamide from water solutions by catalytic photo-oxidation over Fe-pillared clay, Water Res., 185 (2020) 116212, https://doi.org/10.1016/j.watres.2020.116212.
[23] J.X. Zhu, T. Wang, R.L. Zhu, F. Ge, J.M. Wei, P. Yuan, H.P. He, Novel polymer/surfactant modified montmorillonite hybrids and the implications for the treatment of hydrophobic organic compounds in wastewaters, Appl. Clay Sci., 51 (2011) 317–322.
[24] Y.G. Wu, M.C. Yang, S.H. Hu, L. Wang, H.R. Yao, Characteristics and mechanisms of 4A zeolite supported nanoparticulate zero-valent iron as Fenton-like catalyst to degrade methylene blue, Toxicol. Environ. Chem., 96 (2014) 227–242.
[25] W. Najjar, S. Azabou, S. Sayadi, A. Ghorbel, Catalytic wet peroxide photo-oxidation of phenolic olive oil mill wastewater contaminants: Part I. Reactivity of tyrosol over (Al–Fe) PILC, Appl. Catal., B, 74 (2007) 11–18.
[26] H.B. Hadjltaief, M.B. Zina, M.E. Galvez, P. Da Costa, Photo-Fenton oxidation of phenol over a Cu-doped Fe-pillared clay, C.R. Chim., 18 (2015) 1161–1169.
[27] M.M. Bello, A.A. Abdul Raman, A. Asghar, A review on approaches for addressing the limitations of Fenton oxidation for recalcitrant wastewater treatment, Process Saf. Environ. Prot., 126 (2019) 119–140.
[28] E. Rosales, D. Anasie, M. Pazos, I. Lazar, M.A. Sanromán, Kaolinite adsorption-regeneration system for dyestuff treatment by Fenton based processes, Sci. Total Environ., 622–623 (2018) 556–562.
[29] B. Kakavandi, A. Takdastan, S. Pourfadakari, M. Ahmadmoazzam, S. Jorfi, Heterogeneous catalytic degradation of organic compounds using nanoscale zero-valent iron supported on kaolinite: mechanism, kinetic and feasibility studies, J. Taiwan Inst. Chem. Eng., 96 (2019) 329–340.
[30] Y.G. Wu, H.R. Yao, S. Khan, S.H. Hu, L. Wang, Characteristics and mechanisms of kaolinite-supported zero-valent iron/$H_2O_2$ system for nitrobenzene degradation, CLEAN–Soil Air Water, 45 (2017) 1600826, https://doi.org/10.1002/clen.201600826.
[31] S.H. Hu, Y.G. Wu, H.R. Yao, C. Lu, C.J. Zhang, Enhanced Fenton-like removal of nitrobenzene via internal microelectrolysis in nano zerovalent iron/activated carbon composite, Water Sci. Technol., 73 (2016) 153–160.
[32] Y.G. Wu, L. Fan, S.H. Hu, S.C. Wang, H.R. Yao, K.F. Wang, Role of dissolved iron ions in nanoparticulate zero-valent iron/$H_2O_2$ Fenton-like system, Int. J. Environ. Sci. Technol., 16 (2019) 4551–4562.
[33] Y. Wang, J.S. Fang, J.C. Crittenden, C. Shen, Novel RGO/α-FeOOH supported catalyst for Fenton oxidation of phenol at a wide pH range using solar-light-driven irradiation, J. Hazard. Mater., 329 (2017) 321–329.
[34] Y.Y. Liu, X.M. Liu, Y.P. Zhao, D.D. Dionysiou, Aligned α-FeOOH nanorods anchored on a graphene oxide-carbon nanotubes aerogel can serve as an effective Fenton-like oxidation catalyst, Appl. Catal., B, 213 (2017) 74–86.
[35] M.A. Oturan, J.J. Aaron, Advanced oxidation processes in water/wastewater treatment: principles and applications. A review, Crit. Rev. Env. Sci. Technol., 44 (2014) 2577–2641.
[36] J.G. Shi, Z.H. Ai, L.Z. Zhang, Fe@$Fe_2O_3$ core-shell nanowires enhanced Fenton oxidation by accelerating the Fe(III)/Fe(II) cycles, Water Res., 59 (2014) 145–153.
[37] Y.M. Li, Y.Q. Lu, X.L. Zhu, Photo-Fenton discoloration of the azo dye X-3B over pillared bentonites containing iron, J. Hazard. Mater., 132 (2006) 196–201.
[38] E. Guélou, J. Barrault, J. Fournier, J.-M. Tatibouët, Active iron species in the catalytic wet peroxide oxidation of phenol over pillared clays containing iron, Appl. Catal., B, 44 (2003) 1–8.
[39] M. Bobu, A. Yediler, I. Siminiceanu, S. Schulte-Hostede, Degradation studies of ciprofloxacin on a pillared iron catalyst, Appl. Catal., B, 83 (2008) 15–23.
[40] H.H. Huang, M.C. Lu, J. Chen, Catalytic decomposition of hydrogen peroxide and -chlorophenol with iron oxides, Water Res., 35 (2001) 2291–2299.
[41] J. Guo, M. Al-Dahhan, Catalytic wet oxidation of phenol by hydrogen peroxide over pillared clay catalyst, Ind. Eng. Chem. Res., 42 (2003) 2450–2460.
[42] R. Shende, J. Levec, Wet oxidation kinetics of refractory low molecular mass carboxylic acids, Ind. Eng. Chem. Res., 38 (1999) 3830–3837.
[43] M.A. Oturan, M. Pimentel, N. Oturan, I. Sirés, Reaction sequence for the mineralization of the short-chain carboxylic acids usually formed upon cleavage of aromatics during electrochemical Fenton treatment, Electrochim. Acta, 54 (2008) 173–182.
[44] G. Ruppert, R. Bauer, G. Heisler, S. Novalic, Mineralization of cyclic organic water contaminants by the photo-Fenton reaction — influence of structure and substituents, Chemosphere, 27 (1993) 1339–1347.
[45] J.H. Ma, W.J. Song, C.C. Chen, W.H. Ma, J.C. Zhao, Y.L. Tang, Fenton degradation of organic compounds promoted by dyes under visible irradiation, Environ. Sci. Technol., 39 (2005) 5810–5815.
[46] N. Masomboon, C. Ratanatamskul, M.-C. Lu, Chemical oxidation of 2,6-dimethylaniline in the Fenton process, Environ. Sci. Technol., 43 (2009) 8629–8634.
[47] J.H. Ramirez, C.A. Costa, L.M. Madeira, G. Mata, M.A. Vicente, M.L. Rojas-Cervantes, A.J. López-Peinado, R.M. Martín-Aranda, Fenton-like oxidation of orange II solutions using heterogeneous catalysts based on saponite clay, Appl. Catal., B, 71 (2007) 44–56.
[48] C. Catrinescu, C. Teodosiu, M. Macoveanu, J. Miehe-Brendlé, R. Le Dred, Catalytic wet peroxide oxidation of phenol over Fe-exchanged pillared beidellite, Water Res., 37 (2003) 1154–1160.
[49] T. Zhang, J. Ma, Catalytic ozonation of trace nitrobenzene in water with synthetic goethite, J. Mol. Catal. A: Chem., 279 (2008) 82–89.
[50] I.A. Salem, M. El-Maazawi, A.B. Zaki, Kinetics and mechanisms of decomposition reaction of hydrogen peroxide in presence of metal complexes, Int. J. Chem. Kinet., 32 (2000) 643–666.

## Supplementary information

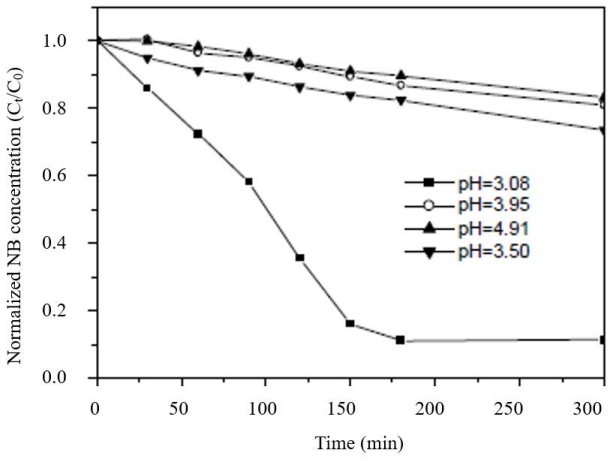


Fig. S1. Influence of initial pH on NB removal by the Fenton-like reaction.